2023-10

Hydrological System and Water Balance of Ungauged Crater Lakes of the Northern Crater Highlands

Lucas, Godwin

Tanzania Journal of Engineering and Technology

https://doi.org/10.52339/tjet.v42i3.954

Tanzania Journal of Engineering and Technology 2023, **42**(**3**): 48-63
OPEN ACCESS articles distributed under Creative Commons Attribution Licence [CC BY-ND]
Websites: https://ajol.org/tjet; https://tjet.udsm.ac.tz

ISSN 1821-536X (**print**); ISSN 2619-8789 (**electronic**)
https://doi.org/10.52339/tjet.v42i3.954

Research Manuscript – First Presented at 2022 Zanzibar Water Conference

Hydrological System and Water Balance of Ungauged Crater Lakes of the Northern Crater Highlands

Godwin Lucas[1 2 4†], Hans Komakech[1 2] , and Ceven Shemsanga[3]

[1]Department of Department of Water and Environmental Science and Engineering, Nelson Mandela African Institution of Science and Technology, P.O. Box 447 Arusha, Tanzania
[2]Water Infrastructure and Sustainable Energy Futures, Nelson Mandela African Institution of Science and Technology, P.O. Box 447 Arusha, Tanzania,
[3]Department of Environmental Engineering and Management, University of Dodoma, P.O. Box 259, Dodoma, Tanzania
[4]Pangani Basin Water Board, Ministry of Water, P.O. Box 7617, Moshi, Tanzania, Email:
[†]Correspondence email address: lucasgodwin7@gmail.com

ABSTRACT

The study aimed to unveil the hydrological system and water balance of the ungauged crater lakes with major focus on the Emakati Lake which occupy 46% of the Empakaai Crater associated to the East African Rift Valley and form part of the Northern Crater Highlands. Water samples for analysis of NO_3^- , Cl^- and stable isotopes (^2H and ^{18}O) were collected from the Emakat lake, springs of the inner, outer and the foot of the Empakaai Crater rims. A combination of satellite data such as digital elevation model (DEM), Climate Hazards Group Infrared Precipitation with Station data (CHIRPS), net shortwave solar radiation, surface temperature, and the computation methods such as Curve Number (CN) Model, DeBruin–Keijman (D-K) Model enabled the computation of water balance components such as Lake level changes, precipitation, runoff and evaporation. Results show that, evaporation (1694.57 mm) surpasses rainfall (878.68 mm) of the Empakaai Crater results of higher enrichments of $\delta^{18}O$ and δ^2H in the lake ranging between 3.28‰ to 3.96‰ and 31.99 to 33.93‰ compared to springs which range between -5.18 to -4.05‰ and -26.62 to -19.48‰ respectively. Springs plots to the left and above of both the GMWL and TMWL, implying that they receive direct recharge from rainfall. The water balance in the area shows that, groundwater flow plays a major role on the lakes hydrological system as it contributes about 22,004,361.12 m^3/year as the groundwater inflow to Emakat Lake which is about 56% of the lake's total inflow and about 22,734,274.00 m^3/year as groundwater outflow which is about 63% of total lake outflow. This imply that, the lake depends less on the weather condition and hence ensuring the sustainability of the ecosystem of the Empakaai crater and the downstream.

ARTICLE INFO

First submitted: **June 29, 2022**

Presented at: **2022 Zanzibar Water Conference,**

1st revised: **Jan. 20, 2023**

2nd revision: **June 15, 2023**

Accepted: **Aug. 4, 2023**

Published: **Oct. 2023**

Keywords: *Emakat Crater lake, lake water balance, stable isotopes of water, ungauged lakes*

INTRODUCTION

The hydrological water balance is a widely used technique in the world to understand

the interaction of components of the hydrological cycle including lakes and their catchments (Zhang et al., 2016; Thapa et al., 2017; Duan et al., 2018). It utilizes the mass conservation principle that gives the input-output relationship of the hydrologic components in an area at a given time which are balanced by the change of storage (Jain & Singh, 2003; UNESCO, 1971). In lakes, water balance provides the quantitative assessment to theoretical and practical hydrological problems such as change predictions in hydrological systems, rational use, distribution of water in time and space, and determination of unknown hydrological components through the analysis of known components (Sokolov & Chapman, 1974).

Hutchinson (1957) classified lakes into 11 main types; one being the crater lakes formed when water permanently occupies a volcanic feature such as a crater or a caldera and may remain active or inactive in influencing the water chemistry (Kusakabe, 1994; Thomas et al., 1996; Rouwet et al., 2015).The water balance of the crater lakes depends largely on the nature of their hydrological system whereby the open lake hydrological system is characterized by surface inflow and outflow while the closed lake hydrological system is characterized by lack of surface inflow and outflow with evaporation and seepage playing a major role in this system (Sokolov & Chapman, 1974; Christenson, 2000).

The current study focuses on the closed ungaguged Emakati Crater Lake, characterized by high pH and dominated by high Na^+ and K^+ ions originating from the weathering of bedrock, hydrothermal reactions, and rainfall (Muzuka et al., 2004; Ryner et al., 2008; Deacampo & Renaut, 2016). Ecological studies (Frame et al., 1975; Childress et al., 2007), and paleoclimate studies (Muzuka et al., 2004; Ryner et al., 2008) undertaken on the Empakaai Crater, suggest the lake's water sources to be the few streams flowing from the inner crater rims, direct precipitation, and groundwater, however, no study undertaken to ascertain this important fact of the lake. Therefore, the current study aimed to unveil the hydrological aspect of Emakat Lake with a major concentration on the water balance, and its interrelationship with the water sources on the outer crater rims including rivers which play major role in supporting the population of the downstrem.

MATERIAL AND METHOD

Description of study area

The Emakat Lake is a crater lake occupying about 46% of the Empakaai Crater which is assocated with the rifting process resulted to the formation of the East African Rift Valley (Gregory) (Muzuka *et al.* 2004; Ryner *et al.* 2006). The lake formed at ca.1.26 Ma when the cratet of the Empakaai was accupied with water. The study area accurs between latitudes ($2^o52'48''S$ and $2^055'48''S$), longitudes ($35^o47'24''E$ and $35^o51'36''E$) at an elevation of about 2300 m above the mean sea level (Figure 1). Bimodal rainfall characterises the lake catchment area which occurs between November and May with a peak in April and May where the annual rainfall ranges between 600 to 1000mm, with spatial variation from the western to eastern slopes respectively, however, the topographical enhancement can result to as high as 1500 mm annual rainfall (Ryner *et al.* 2006; Ryner *et al.* 2008). Annual temperature of the area ranges between 15 to 22ºC while the temperature may fall to below 0^oC on the daily records (Ryner *et al.* 2007). Springs from the outer crater rims drain into the surrounding plains and form major rivers such as Engarasero and Engaruka Rivers, which sustain the population downstream before discharging to Lakes

Natron and Engaruka respectively (Figure 1).

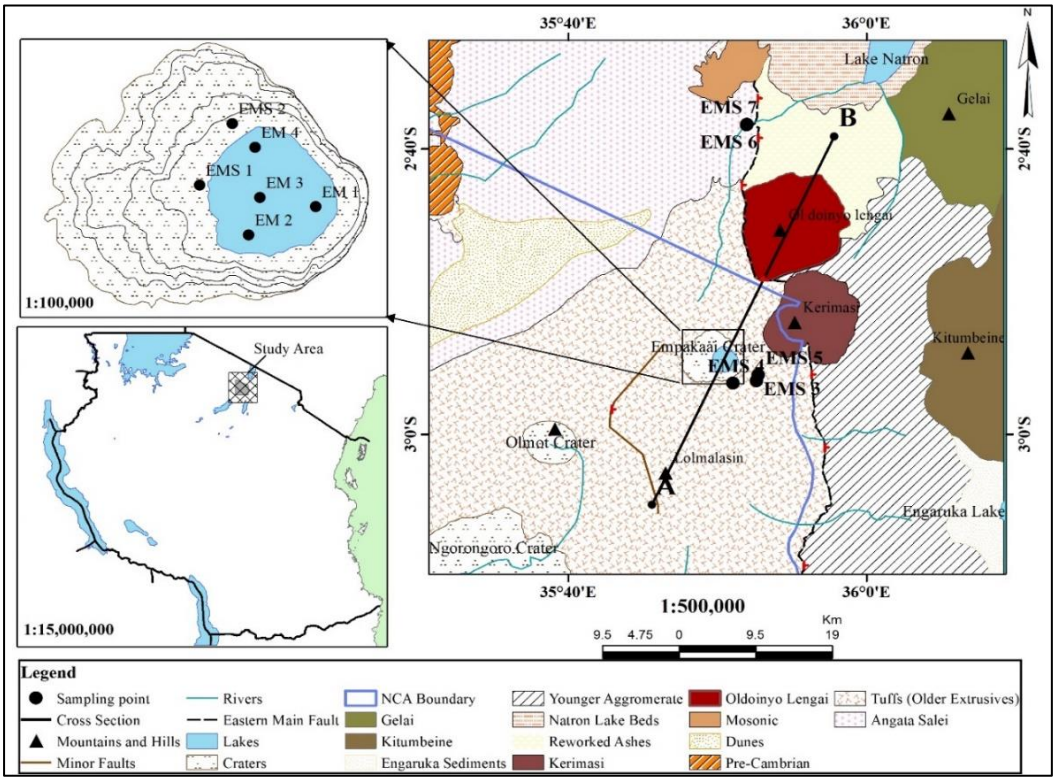

Figure 1: The location and geological map of the study area (modified after Guest et al. 1961).

The hydrogeological study of the Empakaai Crater reveals two aquifers; the upper aquifer composed of fractured phonolite and the lower aquifer composed of nephelinites and mica-augite tuffs where the two aquifers are separated with an aquiclude which is composed of red scoria and tuffs (Heap et *al*. 2014). The aquifers exhibit diverse hydrochemical characteristics where the upper aquifer exhibits fresh water condition while the lower aquifer exhibits saline water of which both form part of the rivers flowing downstream of the Empakaai Crater (Lucas et *al*. 2022).

Sampling and analysis

Sampling at the study area was done in the Emakat lake, springs of the inner, outer and the foot of the Empakaai Crater rims. Precipitation samples were collected at Karatu, located about 45 km south-west of the Empakaai Crater. Sampling for NO_3^- and Cl^- was done in H_2SO_4 acid prewashed 500 ml bottles. Water samples for analysis of stable isotopes (^2H and ^{18}O) were collected using high-density linear polyethylene (HDPE) 100 ml bottles immersed in sampled water ensuring bubble-free and tightened to avoid evaporation. All collected water samples were stored at 4ºC in cooler boxes with ice blocks during fieldwork and in refrigerators before analysis which was performed immediately after the fieldwork.

Standard methods for the analysis of major ions was performed according to Rice *et al.* (2012) whereby Cl^- was analyzed through titration method and NO_3^- was analyzed with the Hatch Spectrophotometer (Dr 2900). Stable water isotopes (δ^2H and $\delta^{18}O$) was done by the Dual Inlet-Isotope Ratio Mass Spectrometer.

Water balance computation methods

Being a closed lake, the large portion of Emakat Lake catchment is located in the inner walls of the Crater and largely depends on precipitation, groundwater, and streamflow from the inner crater walls as inflows and evaporation and groundwater as outflows and hence, its water balance can be computed as in Equation **Error! Reference source not found.**(Sokolov & Chapman 1974).

$$\frac{d}{dt}(S) = P + I_s + I_g - E - O_g \quad (1)$$

where $d/dt(s)$ stands for a change of storage, P for precipitation, I_s and I_g surface and groundwater inflows, E for evaporation, and O_g groundwater outflow.

The lake volume and volume change were calculated from a combination of the digital elevation model (DEM), the topographical map, the bathymetry data, lake surface elevetions collected during sampling and the interannual lake level changes of the Emakat Lake which is 0.4 m (Ryner *et al.* 2008). Since the Empakaai Crater lacks a weather station, rainfall estimation was done using the recently released Climate Hazards Group Infrared Precipitation with Station data (CHIRPS) which has provided the higher resolution rainfall data at 0.05º. The CHIRPS rainfall data was compared with available ground collected data from three weather stations (Monduli, Nainokanoka, and Ngorongoro HQ) in the vicinity of the study area.

The runoff from the Empakaai Crater inner walls was estimated by the Curve Number (CN) Model (Satheeshkumar *et al.* 2017). The DEM image extracted from the United States Geological Survey (USGS) (https://earthexplorer.usgs.gov) was used to delineate the Empakaai Catchment, while Land Use-Land Cover map was obtained from the vegetation cover map of the Empakaai Crater by Ryner *et al.* (2006). The soil map of Tanzania published by the Geological Department, Dodoma Tanzania was retrieved from the European Soil Data Centre (ESDAC) (Samki & Baker 1977).

Evaporation over Emakat Lake was estimated by the DeBruin–Keijman (D-K) Model (Equation **Error! Reference source not found.**). The D-K Model is relevant to lakes that are ungauged like Emakat Lake as it requires few input data which mostly are freely available from online satellite data providers (Duan *et al.* 2018). Moreover, the D-K Model considers the estimation of the heat storage changes which is an important component that can result in large errors if neglected (Duan & Bastiaanssen 2015).

$$E = \frac{\Delta(R_n - Q_t)}{0.85\Delta + 0.63\gamma} \times \frac{86.4}{\lambda\rho_w} \quad (2)$$

The standard density of water ρ_w of 1000 kg/m^3 and the latent heat of vaporization of water (λ) of 2.45 MJ/ kg were used during the evaporation computation (Duan *et al.* 2018). The slope of the saturation curve (Δ) was computed using the monthly average temperature (T) while the psychometric constant (γ) was computed from the atmospheric pressure which is dependent on the altitude (Zotarelli *et al.* 2018) taken to be 2215 meters above the mean sea level for Emakat Lake. The monthly average temperatures were computed from the daily temperature data acquired from the Ngorongoro HQ station. The net short wave solar radiation and surface temperature were obtained freely from https://lpdaac.usgs.gov/ in HDF format then the point data extracted with the aid of the ArcGIS and the python-based algorithm.

In this study, the stable isotopes of water (^{2}H and ^{18}O) were used to compute the inflow-outflow of water to the lake through the isotopic mass balance approach (Özaydin *et al.* 2001). To utilize the isotopic mass balance equation, the isotopic composition of all components of the water balance in Equation **Error! Reference source not found.** were multiplied with the respective component (Equation **Error! Reference source not found.**).

$$\frac{d}{dt}(\delta_L S) = \delta_p P + \delta_p I_s + \delta_g I_g - \delta_E E - \delta_L O_g \quad (3)$$

where the δ_L, δ_p, δ_g, and δ_E are the isotopic composition of the lake, precipitation,

groundwater inflow, and evaporation respectively.

The isotopic composition of the lake and groundwater was estimated as the average of isotopic values (^{2}H and ^{18}O) of samples collected from the lake and springs respectively with the assumption that there exists a negligible annual variation of the isotopic composition of the water balance parameters in the area. Being the most complex component to estimate among the components of the water balance, the isotopic composition of evaporation for Emakat Lake was estimated using the Craig-Gordon (C-G) Evaporation Model (Equation **Error! Reference source not found.**) (Craig & Gordon 1965; Gat *et al.* 2001).

$$\delta_E = \frac{\alpha_{V/L} \times \delta_L - h\delta_A - \varepsilon}{(1-h) + \varepsilon_k} \quad (4)$$

Whereby ε is the effective enrichment factor expressed as $\varepsilon = \varepsilon^* + \varepsilon_k$ by which $\varepsilon^* = (1 - \alpha_{V/L})$ and ε_k is the kinetic isotope fractionation factor resulting from vapor transport through the three layers namely interface, laminar, and turbulent. The δ_A stands for the isotopic composition of the atmosphere while $\alpha_{V/L}$ stands for the isotopic fractionation factor at the vapor-liquid interface.

The isotopic composition of the free atmosphere (δ_A) was obtained from the standardization of the isotopic composition of precipitation with the assumption that local precipitation and atmospheric moisture are obviously in isotopic equilibrium (Horita *et al.* 2008; Özaydin *et al.* 2001). The isotopic equilibrium fractionation factor at the liquid-vapor interface $\alpha_{V/L}$ was computed according to Horita & Wesolowski (1994) while the diffusion-controlled isotope fractionation during water-vapour state change, considered the kinetic fractionation factor (ε_k), was computed according to Horita *et al.* (2008). The groundwater inflow and outflow were consequently computed through the combination of the water balance (Equation **Error! Reference source not found.**) and the isotopic mass balance (Equation **Error! Reference source not found.**) (Özaydin *et al.* 2001). Substite $M = I_g - O_g$ and $N = \delta_g I_g - \delta_L O_g$ in the two equations, then combining to get O_g and I_g, the groundwater outflow (O_g) and groundwater inflow (I_g) to the lake can be estimated by Equations **Error! Reference source not found.** and **Error! Reference source not found.**.

$$O_g = \frac{N - \delta_g M}{\delta_g - \delta_L} \quad (5)$$

and

$$I_g = \frac{N - \delta_L M}{\delta_g - \delta_L} \quad (6)$$

RESULTS AND DISCUSSION

Physical-chemical and isotopic characteristics of Empakaai Crater

The physical-chemical and isotopic composition ($\delta^{18}O$ and $\delta^{2}H$) of the Empakaai Crater are presented in Table 1. The EC of Emakat Lake range from 28,860 to 29,460 µs/cm while those for springs also range from 562 to1584 µs/cm respectively. The concentration of Cl^- and NO_3^- in Emakat Lake ranged between 1014.48 to 1145 mg/L and 92.95 to 224.28 mg/L respectively, whereas for the springs, the ranges were between 2.63 to 154.58 mg/L, and 0.00 to 27.39 mg/L respectively. The stable isotope of the Emakat Lake ranges between 3.28‰ to 3.96‰ with an average of 3.65‰ for $\delta^{18}O$ and range of 31.99 to 33.93‰ with an average of 33.07‰ for $\delta^{2}H$ while the d-excess range between 1.57 and 5.77‰. The isotopic composition of the springs ranges between -5.18 to -4.05‰ with an average of -4.69‰ for $\delta^{18}O$ and -26.62 to -19.48‰ with an average of -23.59‰ for $\delta^{2}H$ while the d-excess ranged from 12.39 to 15.19‰. The isotopic composition of rainfall ranges from -14.2 to 2.52‰ with an average of -8.06‰ for $\delta^{18}O$ and -98.25 to 4.25‰ with an average of 54.37‰ for $\delta^{2}H$.

The isotopic composition of evaporation on the Empakaai Crater is estimated to be 1.47 and 1.09‰ for $\delta^{18}O$ and $\delta^{2}H$ respectively with a d-excess value of 10.70‰ (Table 1).

Table 1:The physical chemical and isotopic composition of the Emakat Lake and the associated springs in the Empakaai Crater

Source Name	Source type	Sample ID	Altitude (m)	Temp ºC	EC µS/cm	NO_3^- mg/L	Cl^- mg/L	18O ‰	D ‰	d-excess ‰
Emakat	Lake	EM 1.1	2215	21.30	29330.00	55.20	1058.69	3.53	33.93	5.69
Emakat	Lake	EM 1.2	2209	20.60	29400.00	52.20	1027.90	3.51	33.58	5.5
Emakat	Lake	EM 2.1	2219	23.20	29100.00	89.50	1065.71	3.96	33.77	2.09
Emakat	Lake	EM 2.2	2204	22.00	29090.00	52.60	1037.45	3.85	32.39	1.59
Emakat	Lake	EM 2.3	2199	21.10	30530.00	80.90	1053.81	3.61	31.02	2.14
Emakat	Lake	EM 3.1	2217	21.00	29390.00	91.00	1014.48	3.64	32.13	3.01
Emakat	Lake	EM 3.2	2202	20.00	29460.00	48.70	1035.33	3.78	33.72	3.48
Emakat	Lake	EM 3.3	2187	18.37	32300.00	141.03	1024.62	3.62	32.35	3.39
Emakat	Lake	EM 4.1	2214	20.60	28860.00	55.80	1145.64	3.28	31.99	5.75
Nguruman	Spring	EMS 1	2219	15.20	562.00	0.90	2.72	-5.18	-26.22	15.22
Oleigero	Spring	EMS 2	2219	15.40	567.00	7.30	7.76	-4.76	-23.19	14.89
Ngopironi	Spring	EMS 3	2162	15.80	670.00	14.00	2.63	-4.52	-23.14	13.02
Marite 1	Spring	EMS 4	2209	15.30	687.00	0.90	10.52	-4.31	-20.29	14.19
Marite 2	Spring	EMS 5	2577	17.70	673.00	1.00	46.31	-4.05	-19.48	12.92
Emparakash 1	Spring	EMS 6	831	25.50	1504.00	14.40	141.90	-5.14	-26.19	14.93
Emparakash 2	Spring	EMS 7	826	24.00	1584.00	5.80	154.58	-4.88	-26.62	12.42
Karatu 1	Rainfall	EMR 1	1575	-	-	-	-	-9.1	-67.2	5.6
Karatu 2	Rainfall	EMR 2	1575	-	-	-	-	-8.1	-56.3	8.5
Karatu 3	Rainfall	EMR 3	1575	-	-	-	-	-14.2	-98.3	15.3
D-K Model	Evaporation	EME 1	-	-	-	-	-	-1.47	-1.09	10.9

The δ^2H and $\delta^{18}O$ characteristics of the Empakaai Crater

The collected data from Emakat Lake and springs and the estimated isotopic data of evaporation were both plotted on the meteoric line graph (Figure 2). The Global Meteoric Water Line (GMWL) was drawn following the equation $\delta^2H = 8\delta^{18}O + 10$ (Levin *et al.* 2009) while the deuterium (δ^2H) and oxygen ($\delta^{18}O$) values for precipitation collected from 1961 to 2016 by the Tanzania Meteorological Agency (TMA) of Dodoma and Dar es salaam were used to plot the Tanzania meteoric Water Line (TMWL). The line yielded an equation of $\delta^2H = 7.2\delta^{18}O + 7.5$. The samples from the Emakat Lake and the springs were plotted on the evaporation line using the equation $\delta^2H = 6.8\delta^{18}O + 8.3$. The slope of the evaporation line for the collected samples (6.8) was less than that of TMWL (7.2) and that of GMWL (8) implying that the d-excess might have been increasing with decreasing δ values (Gonfiantini *et al.* 2001). Samples from Emakat Lake plots were below and to the right of both GMWL and TMWL, implying that there is an enrichment of $\delta^{18}O$ probably due to the evaporation effect as expected in arid regions. The springs plotted to the left and above of both the GMWL and TMWL, implying that they receive direct recharge from rainfall (Levin *et al*. 2009).

The general trend from springs to Emakat lake, however, showed a strong correlation of 0.9899 for $\delta^{18}O$ with EC (Figure 3. C). This suggests that the enrichment of $\delta^{18}O$ on Emakat Lake occurs with increasing evaporation while the springs receive direct recharge from the rainfall and there is a limited time of exposure of surface water before recharging the groundwater and hence no fractionation on the $\delta^{18}O$ during groundwater recharge but rapid enrichment occurs on groundwater upon recharging the Emakat Lake (Talabi & Tijani 2013). Nevertheless, there is a strong positive correlation of $\delta^{18}O$ with NO_3^- 0.9160 (Figure 3.E) while the springs appear to be close to the line, indicating limited evaporation occurs on groundwater while lake water samples are displaced to left and right of the line, indicating that NO_3^- enrichment occurs at a fair constant $\delta^{18}O$ while NO_3^- is reduced at a depth under anaerobic environment (Talabi & Tijani 2013).

There is a limited variation of Cl^- versus δ^2H on both Emakat Lake and its associated springs (Figure 3.F) which can be associated to partial removal of Cl^- to solid-phase during mineral crystallization as a result of the evaporation process on the lake and evapotranspiration process which tends to concentrate salts in groundwater without fractionation of stable isotopes (Armienta *et al.* 2008; Flow *et al.* 2015).

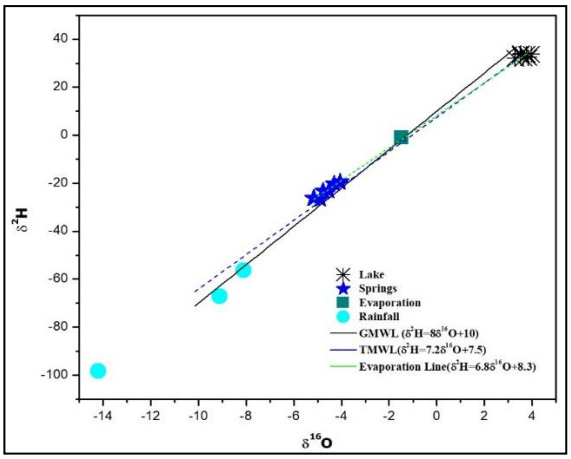

Figure 2: Graph showing isotopic variation of δ^2H Versus $\delta^{18}O$ along the Global (GMWL) and Tanzania (TML) Meteoric lines.

The d-excess variation against $\delta^{18}O$ shows that despite the negative correlation of -0.9749 (Figure 3.D), there still occur different behaviors among different water sources. The positive correlation of 0.3332 for d-excess versus δ^2H on the Emakat Lake and the negative correlation of -0.2377 for the associated springs (Figure 3.G & F) may be due to higher evaporative effect occurring on Emakat Lake and the slight evaporative effects on the associated springs (Talabi & Tijani 2013). The implication of the hydrochemical characteristics and d-excess of Emakat Lake with its associated springs to their respective $\delta^{18}O$ and δ^2H reflects their position on the GMWL, whereby higher evaporation effects result in higher enrichment of $\delta^{18}O$ and δ^2H of the Emakat

Lake occurs. Groundwater is subjected to limited evaporative effects and receives direct recharge from rainfall, however deviation from GMWL to TMWL is ascribed to secondary evaporative effects of groundwater, modification during rock-water interaction and recharge from the Emakat Lake (Karolyte *et al*. 2017).

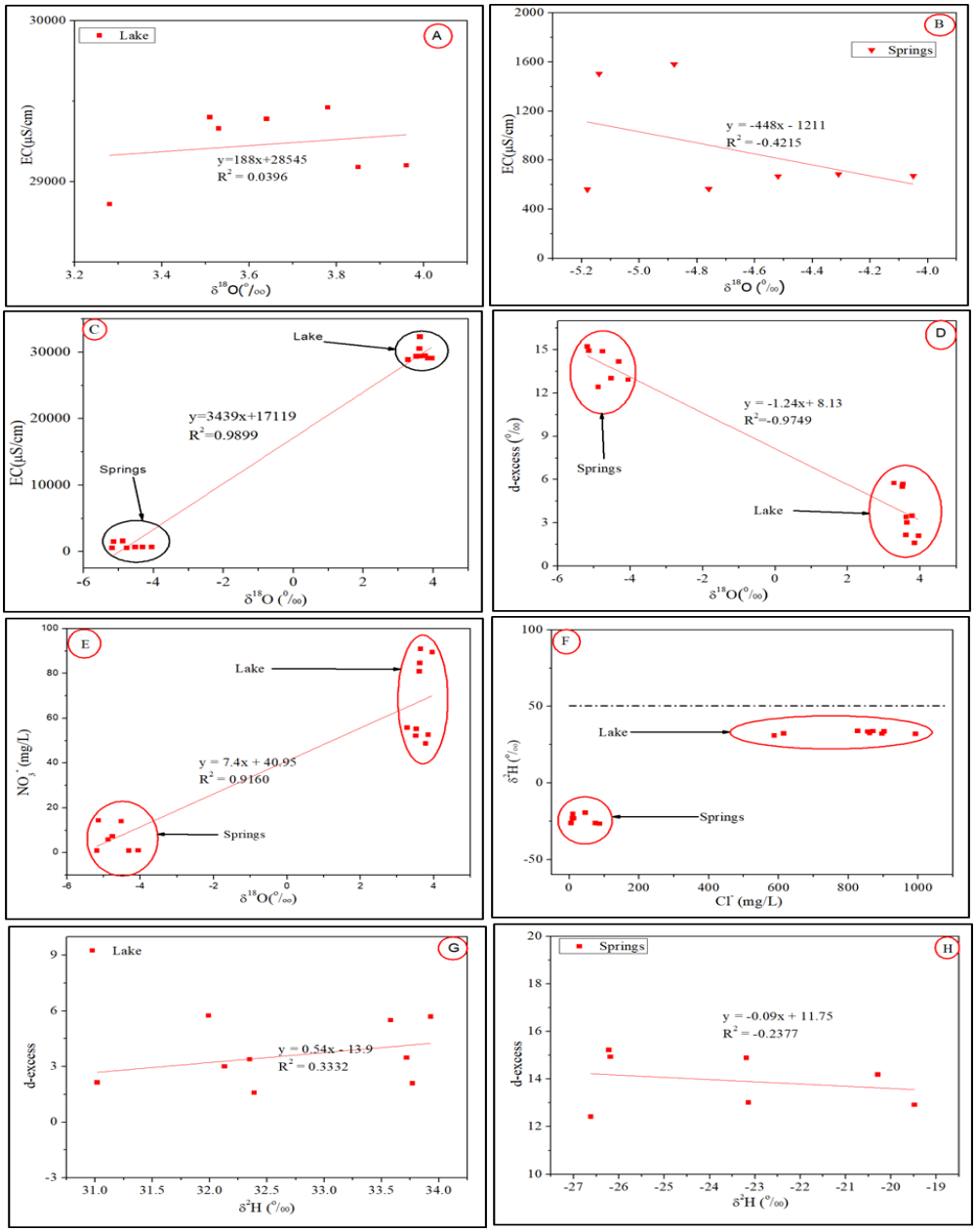

Figure 3: Variation of δ^2H and $\delta^{18}O$ with physicochemical parameters of the Emakat Lake and associated springs.

Emakat Lake Volume Change

The estimation of Emakat Lake volume changes from the combination of the DEM, bathymetric survey, GPS coordinates, and the inter-annual lake volume changes of 0.4 m according to Ryner et al. (2008) resulted in an average maximum and minimum lake water levels of 2216.57 MAMSLand 2216.17 MAMSL respectively. This resulted in a maximum volume of 292,564,175.58 m^3 and a minimum lake volume of 289,515,085.03 m^3 attained in the rainy and dry seasons respectively, hence, an annual lake water volume change of 3,049,090.55 m^3.

Rainfall

The validation and performance evaluation of the CHIRPS data by Dinku *et al.* (2018) concluded that the resource has higher performance over East Africa including Tanzania. However, the validation results of CHIRPS data performed better at the Nainokanoka station (station close to the study area) for the the R^2 test by 0.8527 (

Table 2) on the average monthly data compared to other tests. This suggests that the CHIRPS data in the study area can perform better on the prediction of the monthly average rainfall over a range of years' time series. The average CHIRPS annual rainfall obtained is 878.68 mm (

Table 5) for the Empakaai Crater which falls in the same range of 600 to 1000 mm annual rainfall for the Crater Highlands (Ryner *et al.* 2006).

Table 2: Data performance for validation of the CHIRPS data with three stations; Ngorongoro HQ for 2013 to 2018, Nainokanoka for 2006, 2007, 2013, 2014, 2017 and 2018, and Monduli for 2012 to 2016.

Station	Ngorongoro HQ	Nainokanoka	Monduli
R^2(Monthly Rainfall)	0.1072	0.2321	0.514
R^2(Average Monthly Rainfall)	0.6954	0.8527	0.7974

Runoff

The LU/LC map of the Empakaai Crater was obtained from the vegetation type classified according to Ryner et al. (2006), which are montane forest about 10%, wooded grassland about 40%, and the highland shrubs (thickets) about 50% (Figure 4.A). The Empakaai Crater is covered by volcanic soil classified as the Eutric Nitosol which forms through free drainage in an area with rainfall between 750 to 1000 mm and temperature between 13 and 15ºC while its thickness range above 50 cm (Samki & Baker, 1977).

The soil sample collected from the Empakaai Crater indicated that it is sandy loam with 71.59% sand, 17.78% silt, and 10.63% clay (

). The soil classification at Empakaai Crater exhibited a moderately high infiltration rate and hence a low runoff coefficient (Ross et al., 2018).

Table 3: Analysis results for the soil sample collected at Empakaai Crater

Sample Name	Parameter	Description
Empakaai Soil Sample 1	Sand	71.59
	Silt	17.78%
	Clay	10.63%
	Textural Class	Sandy Loam

	Average Moisture Content	31.60%

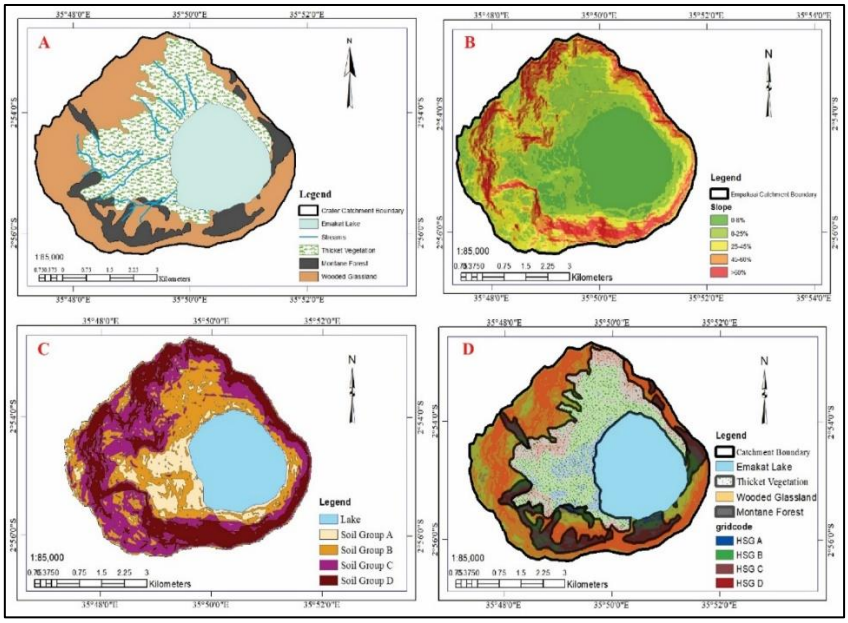

Figure 4: The maps of Empakaai Crater Showing (A) The LU/LC based on vegetation distribution; (B) The slope classification obtained from DEM, (C) The hydrologic soil groups (HSG) classification, (D) The three hydrological soil cover complexes

Table 4: Weighted curve number calculation from the hydrological soil-cover complex

Land Cover		Soil Group	CN	AMC	Area (m^2)	CNxArea
Vegetation	**Hydrological Condition**					
Thicket Vegetation	Good	B	58	AMC II	6,462,360.53	374,816,910.87
	Good	C	71	AMC II	2,640,116.48	187,448,270.23
	Good	A	30	AMC II	1,911,959.97	57,358,799.18
	Good	D	78	AMC II	1,360,710.14	106,135,390.73
Wooded Grassland	Fair	B	65	AMC II	2,972,711.20	193,226,228.17
	Fair	C	76	AMC II	4,634,527.87	352,224,118.11
	Fair	A	43	AMC II	484,319.36	20,825,732.33
	Fair	D	82	AMC II	6,098,554.27	500,081,450.42
Montane Forest	Good	B	55	AMC II	55,581.51	3,056,983.23
	Good	B	55	AMC II	464,976.69	25,573,717.81
	Good	B	55	AMC II	138,011.38	7,590,626.07
	Good	B	55	AMC II	214,285.29	11,785,690.93
	Good	B	55	AMC II	253,948.83	13,967,185.54
	Good	B	55	AMC II	6,985.85	384,221.56
	Good	C	70	AMC II	188,374.95	13,186,246.47
	Good	C	70	AMC II	727,892.10	50,952,447.06
	Good	C	70	AMC II	17,968.34	1,257,783.76

Land Cover		Soil Group	CN	AMC	Area (m^2)	CNxArea
Vegetation	Hydrological Condition					
	Good	C	70	AMC II	168,831.15	11,818,180.42
	Good	C	70	AMC II	189,392.44	13,257,470.87
	Good	C	70	AMC II	6,168.14	431,770.10
	Good	C	70	AMC II	13,779.49	964,564.39
	Good	A	30	AMC II	794.03	23,820.83
	Good	A	30	AMC II	14,611.66	438,349.87
	Good	A	30	AMC II	81,088.98	2,432,669.27
	Good	A	30	AMC II	130,277.06	3,908,311.88
	Good	A	30	AMC II	22,097.48	662,924.38
	Good	D	77	AMC II	94,041.64	7,241,206.13
	Good	D	77	AMC II	873,594.48	67,266,775.26
	Good	D	77	AMC II	701.09	53,983.85
	Good	D	77	AMC II	442,955.29	34,107,557.13
	Good	D	77	AMC II	243,660.37	18,761,848.66
	Good	D	77	AMC II	90,954.73	7,003,514.59
	Good	D	77	AMC II	45,832.16	3,529,076.15
				Sum	**31,052,064.96**	**2,091,773,826.24**
					Weighted Curve Number	**67.36**
					Potential Maximum Retention after runoff begins (S)	**109.70**

The combination of the soil characteristics and the slope classification (Figure 4. B) done from the DEM, resulted to the HSG map (Figure 4. C) where HSG identified are HSG A, HSG B, HSG C, and HSG D. A combination of the land-use map and the HSG map resulted into three hydrological soil-cover complexes (Figure 4. D). A summary of the obtained hydrologic soil-cover complex with their respective curve numbers is presented in Table 4. The area of each hydrological unit in the hydrological soil-cover complex was calculated, the respective CN was identified, and hence a weighted CN of 67.36 potential maximum retention after runoff begins of 109.70 which resulted to runoff of 332.42 mm (Table 4 & 5).

Evaporation

The evaporation over the Emakat Lake computed by the D-K model utilized ρ_w of 1000 kg/m^3 and the λ of 2.45 MJ/ kg (Duan et al. 2018). The slope of the saturation curve (Δ) was computed using the monthly average temperature (T) while the psychometric constant (γ) was computed from the atmospheric pressure which is dependent on the altitude (Zotarelli et al. 2018), and the altitude of 2215 MAMSLwas used for Emakat Lake. The annual evaporation from Emakat Lake was established to be1694.57 mm (

Table 5).

Table 5: Summary of the computation results for evaporation, rainfall and runoff from Empakaai

Month	Air temperature		Surface temperature	Shortwave radiation	Extra-terrestrial Radiation	Net Radiation	Evaporation	Rainfall
	Tmin(ºC)	Tmax(ºC)	To(ºC)	Rs(W/m2)	Ra (W/m2)	Rn(W/m2)	(mm)	(mm)
January	7.09	17.47	20.29	695.11	432.05	483.38	175.65	77.26
February	10.44	18.81	20.18	805.08	441.89	564.42	141.36	77.05
March	16.72	23.11	19.75	678.78	440.37	475.29	187.84	133.42
April	12.01	17.08	15.91	546.28	419.64	375.77	166	247.14
May	12.56	16.96	16.31	409.61	390.76	273.82	169.63	57.71
June	11.42	16.56	17.23	405.61	373.94	266.01	24.84	20.11
July	8.97	14.49	17.98	488.7	380.86	323.12	89.27	8.19
August	8.97	16.69	19.88	603.82	405.81	409.96	136.78	10.53
September	9.49	19.06	21.8	793.57	430.35	551.05	228.93	5.46
October	10.06	18.27	22.93	646.77	438.89	452.33	163.26	31.07
November	9.42	20.11	20.69	682.88	432.85	475.19	51.91	105.97
December	6.99	16.54	18.43	529.4	427.04	366.56	159.12	104.77
Total Annual							**1694.57**	**878.68**

Water balance of Emakat Lake

The water balance of Emakat Lake shows that groundwater flow plays a major role in the lake's water balance with a total of 22,004,361.12 m^3/year as the groundwater inflow to Emakat Lake which is about 56% of the lake's total inflow and about 22,734,274.00 m^3/year as groundwater outflow which is about 63% of total lake outflow (

Table **6**). The major lake withdrawals include groundwater outflow and evaporation but groundwater outflow, however, surpasses evaporation by 26%. The major inflows are groundwater inflow (56%), runoff from crater walls (26%), and direct precipitation (18%) of the total inflows. The higher percentage ratio of contribution to lake inflow and outflow implies that the lake depends less on the weather condition as reported in previous studies (Ryner *et al.*, 2007; Ryner *et al.*, 2008), instead, the drop in its level is due to its tendency to balance the evaporation which surpasses rainfall. The higher groundwater outflow might have a higher contribution to the Engaresero and Engaruka Rivers which originate from the outer crater rims of the Empakaai Crater and support the life of the downstream residents.

Table 6. Summary of the isotopic mass balance for estimation of the groundwater flow

Parameter	Volume (m^3/year)	Isotopic ($\delta^{18}O$)	Isotopic ($\delta^{2}H$)	Percentage (%)
Lake Volume Change	3,049,090.56	3.65	33.07	
Precipitation over the Lake	7,063,956.54	-10.49	-73.90	18%
Runoff from Crater Walls	10,322,309.68	-10.49	-73.90	26%
Springs inflow from Crater Walls	15,768.00	-4.75	-23.23	0%
Evaporation	13,623,030.78	-1.64	-1.12	37%
Groundwater inflow	22,004,361.12	-4.69	-23.59	56%
Groundwater Outflow	22,734,274.00	3.65	33.07	63%

CONCLUSION AND RECOMMENDATION

The higher evaporation (1694.57 mm) that surpasses rainfall (878.68 mm) of the Empakaai Crater results in increase of the solute concentration of Emakat Lake including enrichments of $\delta^{18}O$ and $\delta^{2}H$ in the lake ranging between 3.28‰ to 3.96‰ and 31.99 to 33.93‰ compared to springs which range between -5.18 to -4.05‰ and -26.62 to -19.48‰ respectively. The Emakat Lake is subjected to higher evaporation effect which results to enrichment of enrichment of $\delta^{18}O$ hence plots below and to the right of both GMWL and TMWL while springs plots to the left and above of both the GMWL and TMWL, implying that they receive direct recharge from rainfall. The d-excess of the study area increase with decreasing δ values as a result the evaporation line of the Emakat Lake and the springs of the Empakaai Crater plots which is 6.8 to be less than that of TMWL (7.2) and that of GMWL (8).The general strong correlation of 0.9899 for $\delta^{18}O$ with EC suggests that, enrichment of $\delta^{18}O$ on Emakat Lake occurs with increasing evaporation while the springs receive direct recharge from the rainfall and there is a limited time of exposure of surface water before recharging the groundwater and hence no fractionation on the $\delta^{18}O$ during groundwater recharge.

Limited evaporation occurs on springs as indicated by the strong positive correlation of 0.9160 for $\delta^{18}O$ and NO_3^- with their plots to be close to the line, while the lake water plots are displaced to the left and right of the line, indicating that NO_3^- enrichment occurs at a fair constant $\delta^{18}O$ while NO_3^- is reduced at a depth under anaerobic environment. Limited variation of Cl^- versus $\delta^{2}H$ on both Emakat Lake and its associated springs is associated to partial removal of Cl^- to solid-phase during mineral crystallization as a result of the evaporation process on the lake and evapotranspiration process which tends to concentrate salts in groundwater without fractionation of stable isotopes.

Groundwater flow plays a major role on the lakes sustainability as it contributes about 22,004,361.12 m^3/year as the groundwater inflow to Emakat Lake which is about 56% of the lake's total inflow and about 22,734,274.00 m^3/year as groundwater outflow which is about 63% of total lake outflow. Other components include evaporation (37%), runoff from crater walls (26%), and direct precipitation (18%). The higher percentage ratio of contribution to lake inflow and outflow implies that the lake depends less on the weather condition while the drop in its level is due to its tendency to balance the evaporation which surpasses rainfall. The higher groundwater outflow has a higher contribution to the Engaresero and Engaruka Rivers which originate from the

outer crater rims of the Empakaai Crater and support the life of the downstream residents. Therefore, the life of the ecosystem of the Empakaai crater and the downstream depends on the sustainability of the hydrological system and water balance of the Emakat Lake.

Acknowledgment

The authors would like to acknowledge the Centre for Water Infrastructure and Sustainable Energy Futures (WISE–Futures), the African center of excellence hosted by the Nelson Mandela African Institution of Science and Technology for financial support.

REFERENCES

Childress, B., Hughes, B., Harper, D. and van den Bossche, W. (2007). East African flyway and key site network of the Lesser Flamingo (Phoenicopterus minor) documented through satellite tracking Ostrich-Journal of African Ornithology, 78(2), 463–468.

Christenson, B. W. (2000). Geochemistry of fluids associated with the 1995-1996 eruption of Mt. Ruapehu, New Zealand: Signatures and processes in the magmatic-hydrothermal system Journal of Volcanology and Geothermal Research, 97(1–4), 1–30. https://doi.org/10.1016/S0377-0273(99)00167-5

Craig, H. and Gordon, L. (1965). Craig-Gordon Pisa D and O-18 in the ocean and the marine atmosphere.pdf.

Deacampo, M. D. and Renaut, W. R. (2016). Soda lakes of East Africa Soda Lakes of East Africa, February, 1–408. https://doi.org/10.1007/978-3-319-28622-8.

Dinku, Tufa, Funk, C., Peterson, P., Maidment, R., Tadesse, T., Gadain, H. and Ceccato, P. (2018). Validation of the CHIRPS satellite rainfall estimates over eastern Africa Quarterly Journal of the Royal Meteorological Society, 144(August), 292–312. https://doi.org/10.1002/qj.3244.

Duan, Z. and Bastiaanssen, W. G. M. (2015). A new empirical procedure for estimating intra-annual heat storage changes in lakes and reservoirs: Review and analysis of 22 lakes Remote Sensing of Environment, 156, 143–156. https://doi.org/10.1016/j.rse.2014.09.009

Duan, Z., Gao, H. and Ke, C. (2018). Estimation of lake outflow from the poorly gauged Lake Tana (Ethiopia) using satellite remote sensing data Remote Sensing, 10(7), 1–21. https://doi.org/10.3390/rs10071060

Flow, G., Park, N., Hedley, P., Dogramaci, S. and Dodson, W. (2015). The Use of Major Ion Analysis and Stable Isotopes O18 and H2 to Distinguish The Use of Major Ion Analysis and Stable Isotopes O 18 and H 2 to Distinguish Groundwater Flow in Karijini National Park , Western Australia February.

Frame, G., Frame, L. H. and Spillett, J. J. (1975). An ecological survey and development plan for the Empakaai Crater ecosystem (Ngorongoro Conservation Area) Serengeti Research Contribution, 212, 472.

Gat, J. R., Mook, W. G. and Meijer, H. A. J. (2001). Environmental isotopes in the hydrological cycle Principles and Applications UNESCO/IAEA Series, 2, 63–67.

Gonfiantini, R., Roche, M., Olivry, J., Fontes, J. and Maria, G. (2001). The altitude effect on the isotopic composition of tropical rains.

Heap, M. J., Baud, P., Meredith, P. and Vinciguerra, S. (2014). The permeability and elastic moduli of tuff from Campi Flegrei , Italy : Implications for ground deformation modelling The permeability and elastic moduli of tuff from Campi Flegrei , Italy : implications for ground deformation modelling. January. https://doi.org/10.5194/se-5-25-2014

Horita, J., Rozanski, K. and Cohen, S. (2008). Isotopes in Environmental and Health Studies Isotope effects in the evaporation of water: a status report of the Craig–Gordon model Isotope effects in the evaporation of water: a status report of the Craig–Gordon model Isotopes in Environmental and Health Studies, 44(1), 23–49. https://doi.org/10.1080/10256010801887174

Horita, J. and Wesolowski, D. J. (1994). Horita and Wesolowski 1994 58(16), 1–13. papers2://publication/uuid/F9BCD32F-8569-4ACF-81AF-08518BF40A32

Hutchinson, G. E. 1957 A Treatise on Limnology. Vol 1: Georgraphy, Physics and Chemistry John Wiley & Sons

Jain, S. . and Singh, V. P. (2003). Chapter 10 Reservoir sizing Developments in Water Science. https://doi.org/10.1016/S0167-5648(03)80064-3

Kusakabe, M. (1994). Geochemistry of Crater Lakes Preface Geochemical Journal, 28(3), 137–138.

Levin, N. E., Zipser, E. J. and Cerling, T. E. (2009). Isotopic composition of waters from Ethiopia and Kenya : Insights into moisture sources for eastern Africa 114(September), 1–13. https://doi.org/10.1029/2009JD012166

Lucas, G., Komakech, H. and Shemsanga, C. (2022). Hadrochemical characteristics of crater lakes and their influence on the downstream water supply sources; Emakat Lake, Northern Tanzania as a case study [Manuscript in preparation]. Department of Water and Environmental Science and Engineering, Nelson Mandela African Institution of Science and Technology.

Muzuka, A. N. N., Ryner, M. and Holmgren, K. (2004). 12,000-Year, preliminary results of the stable nitrogen and carbon isotope record from the Empakai Crater lake sediments, Northern Tanzania Journal of African Earth Sciences, 40(5), 293–303. https://doi.org/10.1016/j.jafrearsci.2004.12.005

Özaydin, V., Şendil, U. and Altinbilek, D. (2001). Stable isotope mass balance method to find the water budget of a lake Turkish Journal of Engineering and Environmental Sciences, 25(4), 329–344. https://doi.org/10.1128/JVI.00693-11

Rice, E. W., Baird, R. B., Eaton, A. D. and Clesceri, L. S. (2012). Standard methods for the examination of water and wastewater (Vol. 10) American Public Health Association Washington, DC.

Ross, C. W., Prihodko, L., Anchang, J., Kumar, S., Ji, W. and Hanan, N. P. (2018). HYSOGs250m, global gridded hydrologic soil groups for curve-number-based runoff modeling Scientific Data, 5(May), 180091. https://doi.org/10.1038/sdata.2018.91

Rouwet, D., Christenson, B., Tassi, F. and Vandemeulebrouck, J. (2015). Volcanic lakes In Volcanic Lakes (Issue March). https://doi.org/10.1007/978-3-642-36833-2

Ryner, M. A., Bonnefille, R., Holmgren, K. and Muzuka, A. (2006). Vegetation changes in Empakaai Crater, northern Tanzania, at 14,800-9300 cal yr BP Review of Palaeobotany and Palynology, 140(3–4), 163–174. https://doi.org/10.1016/j.revpalbo.2006.03.006

Ryner, M., Gasse, F., Rumes, B. and Verschuren, D. (2007). Climatic and hydrological instability in semi-arid equatorial East Africa during the late Glacial to Holocene transition: A multi-proxy reconstruction of aquatic ecosystem response in northern Tanzania Palaeogeography, Palaeoclimatology, Palaeoecology, 248(3–4), 440–458. https://doi.org/10.1016/j.palaeo.2006.12.014

Ryner, Maria, Holmgren, Æ. K. and Taylor, Æ. D. (2008). A record of vegetation dynamics and lake level changes from Lake Emakat , northern Tanzania , during the last c . 1200 years 583–601. https://doi.org/10.1007/s10933-007-9184-0

Samki, J. and Baker, R. (1977). Provisional Soils Map of Tanzania Geological Survey Department, Dodoma.http://eusoils.jrc.ec.europa.eu/esdb_archive/eudasm/africa/maps/afr_tz2003_so.htm

Satheeshkumar, S., Venkateswaran, S. and Kannan, R. (2017). Rainfall–runoff estimation using SCS–CN and GIS approach in the Pappiredipatti watershed of the Vaniyar sub basin, South India Modeling Earth Systems and Environment, 3(1), 1–8.

https://doi.org/10.1007/s40808-017-0301-4

Sokolov, A. and Chapman, T. G. (1974). Methods for water balance computations; an international guide for research and practice In Journal of Environmental Science and Technology (Vol. 23, Issue March). https://doi.org/10.1017/CBO9781107415324.004

Talabi, A. O. and Tijani, M. N. (2013). Hydrochemical and stable isotopic characterization of shallow groundwater system in the crystalline basement terrain of Ekiti area, southwestern Nigeria Applied Water Science, 3(1), 229–245. https://doi.org/10.1007/s13201-013-0076-3

Thapa, B. R., Ishidaira, H., Pandey, V. P. and Shakya, N. M. (2017). A multi-model approach for analyzing water balance dynamics in Kathmandu Valley, Nepal Journal of Hydrology: Regional Studies, 9, 149–162. https://doi.org/10.1016/j.ejrh.2016.12.080

Thomas, R., Meybeck, M. and Beim, A. (1996). Lakes Water Quality Assessments - A Guide to Use of Biota, Sediments and Water in Environmental Monitoring, 5.

UNESCO (1971). Scientific framework of world w a t e r balance Unesco.

Zhang, Z., Huang, Y., Xu, C. Y., Chen, X., Moss, E. M., Jin, Q. and Bailey, A. M. (2016). Analysis of Poyang Lake water balance and its indication of river–lake interaction SpringerPlus, 5(1). https://doi.org/10.1186/s40064-016-3239-5

Zotarelli, L., Dukes, M. D., Romero, C. C., Migliaccio, K. W. and Kelly, T. (2018). Step by Step Calculation of the Penman-Monteith Evapotranspiration (FAO-56 Method) 1, 1–10.